consistent with a role for PKG in LTP, and suggest that under some circumstances cGMP analogues can also activate other mechanisms that may be involved in long-term depression.

The present results suggest that soluble guanylyl cyclase and PKG are involved in the induction of LTP and could serve as target proteins for retrograde messengers. Consistent with this idea, recent studies indicate that 8-Br-cGMP increases both the amplitude of evoked excitatory postsynaptic currents (e.p.s.cs) and the frequency of miniature e.p.s.cs in hippocampal cultures[21], suggesting that cGMP acts presynaptically. However, postsynaptic mechanisms may also be involved. cGMP and PKG have also been shown to produce activity-dependent long-lasting effects in cerebellum and sensory-motor cortex[22–24]. Because these effects are implicated in procedural learning[25,26], whereas LTP in hippocampus is thought to be involved in declarative learning[27], it is possible that these different types of learning at the behavioural level may involve, in part, similar underlying biochemical mechanisms. □

Received 16 September 1993; accepted 18 March 1994.

1. Verma, A., Hirsch, D. J., Glatt, C. E., Ronnett, G. V. & Snyder, S. H. *Science* **259,** 381–384 (1993).
2. DeVente, J. & Steinbusch, H. W. *Acta Histochem.* **92,** 13–38 (1992).
3. Haley, J. E., Wilcox, G. L. & Chapman, P. F. *Neuron* **8,** 211–216 (1992).
4. East, S. J. & Garthwaite, J. *Neurosci. Lett.* **123,** 17–19 (1991).
5. Chetkovich, D. M., Klann, E. & Sweatt, J. D. *Neuro Report* **4,** 919–922 (1993).
6. Hawkins, R. D., Zhuo, M. & Arancio, O. *J. Neurobiol.* (in press).
7. Bliss, T. V. P. & Collingridge, G. L. *Nature* **361,** 31–39 (1993).
8. Zhuo, M., Small, S. A., Kandel, E. R. & Hawkins, R. D. *Science* **260,** 1946–1950 (1993).
9. Stevens, C. F. & Wang, Y. Y. *Nature* **364,** 147–149 (1993).
10. Snider, R. M., McKinney, M., Forray, C. & Richelson, E. *Proc. natn. Acad. Sci. U.S.A.* **81,** 3905–3909 (1984).
11. Garthwaite, J., Charles, S. L. & Chess-Williams, R. *Nature* **326,** 385–388 (1988).
12. Fleisch, J. H. *et al. J. pharmac. exp. Ther.* **229,** 681–689 (1984).
13. Schultz, C. *et al. J. biol. Chem.* **268,** 6316–6322 (1993).
14. Schulz, S., Yuen, P. S. T. & Garbers, D. L. *Trends pharmac. Sci.* **12,** 116–120 (1991).
15. White, R. E. *et al. Nature* **361,** 263–266 (1993).
16. Tsou, K., Snyder, G. L. & Greengard, P. *Proc. natn. Acad. Sci. U.S.A.* **90,** 3462–3465 (1993).
17. Schlichter, D. J., Casnellie, J. E. & Greengard, P. *Nature* **273,** 61–62 (1978).
18. Frey, U., Huang, Y.-Y. & Kandel, E. R. *Science* **60,** 1661–1664 (1993).
19. Geiger, J., Nolte, D., Butt, E., Sage, S. O. & Water, U. *Proc. natn. Acad. Sci. U.S.A.* **89,** 1031–1035 (1992).
20. Wigström, H., Gustafsson, B., Huang, Y.-Y. & Abraham, W. C. *Acta physiol. scand.* **126,** 317–319 (1986).
21. Arancio, O., Kandel, E. R. & Hawkins, R. D. *Soc. Neurosci. Abstr.* **19,** 241 (1993).
22. Shibuki, K. & Okada, D. *Nature* **349,** 326–328 (1991).
23. Ito, M. & Karachot, L. *Neuroreport* **1,** 129–132 (1990).
24. Woody, C. D., Swartz, B. E. & Gruen, E. *Brain Res.* **158,** 373–395 (1978).
25. Ito, M. *A. Rev. Neurosci.* **12,** 85–102 (1989).
26. Brons, J. F. & Woody, C. D. *J. Neurophysiol.* **44,** 605–615 (1980).
27. Squire, L. R. & Zola-Morgan, S. *Science* **253,** 1380–1386 (1991).
28. Zhuo, M., Kandel, E. R. & Hawkins, R. D. *Neuro Report* (in the press).

ACKNOWLEDGEMENTS. We thank D. Sweatt for providing the protocol for the protein kinase assay, R. Y. Tsien, D. V. Madison and S. Siegelbaum for their comments on an earlier draft, S. Mack and C. Lam for preparing the figures and A. Krawetz and H. Ayers for typing the manuscript. This work was supported in part by grants from the National Institute on Aging, the National Institute of Mental Health and the Howard Hughes Medical Institute.

Limb alterations in *brachypodism* mice due to mutations in a new member of the TGFβ-superfamily

Elaine E. Storm*, Thanh V. Huynh†, Neal G. Copeland‡, Nancy A. Jenkins‡, David M. Kingsley*§ & Se-Jin Lee†

* Department of Developmental Biology, Beckman Center B300, Stanford University School of Medicine, Stanford, California 94305-5427, USA
† Department of Molecular Biology and Genetics, Johns Hopkins University School of Medicine, 725 North Wolfe St, Baltimore, Maryland 21205, USA
‡ Mammalian Genetics Laboratory, ABL Basic Research Program, NCI Frederick Cancer Research and Development Center, PO Box B, Frederick, Maryland 21702-1201, USA

THE mutation *brachypodism* (*bp*) alters the length and number of bones in the limbs of mice but spares the axial skeleton[1,2]. It illustrates the importance of specific genes in controlling the morphogenesis of individual skeletal elements in the tetrapod limb[3,4]. We now report the isolation of three new members of the transforming growth factor-β (TGF-β) superfamily[5] (growth/differentiation factors (GDF) 5, 6 and 7) and show by mapping, expression patterns and sequencing that mutations in *Gdf5* are responsible for skeletal alterations in *bp* mice. GDF5 and the closely related GDF6 and GDF7 define a new subgroup of factors related to known bone- and cartilage-inducing molecules, the bone morphogenetic proteins (BMPs)[6]. Studies of *Bmp5* mutations in *short ear* mice have shown that at least one other BMP gene is also required for normal skeletal development[7]. The highly specific skeletal alterations in *bp* and *short ear* mice suggest that different members of the BMP family control the formation of different morphological features in the mammalian skeleton.

The *bp* mutation acts cell non-autonomously *in vitro* and *in vivo*, and may disrupt production of a signal that stimulates mesenchyme aggregation and chondrogenesis in limbs[8,9]. To test whether the skeletal alterations in brachypod mice could be due to mutations in a member of the BMP family of secreted signalling molecules we determined the mouse chromosome map locations of several BMP and BMP-related genes. The previously described *Op1*/(*Bmp7*)[10,11] and *Op2*/(*Bmp8*)[12] genes both map outside the candidate interval for the *bp* mutation, as do the genes for *Bmp2* -*Bmp6* (refs 7, 13).

Three new BMP-related factors were identified by degenerate polymerase chain reaction (PCR; Fig. 1) and designated GDF5, GDF6 and GDF7. Like other BMPs and TGF-β superfamily members, each of the new factors contains a putative polybasic proteolytic processing site followed by a carboxy-terminal region containing seven conserved cysteine residues[5]. Previously characterized BMPs fall into three homology groups[6,12]: the BMP2/BMP4 subfamily; the Vgr1(BMP6)/OP1(BMP7)/BMP5/OP2(BMP8) subfamily; and BMP3. Molecules within each group share 74–92% identity in the amino-acid sequence of the mature C-terminal signalling region. Members of different subfamilies share 40–60% identity. With the exception of a 26-amino-acid glycine-rich insert present in GDF7, GDF5, GDF6 and GDF7 share 80–86% identity with each other in the mature C-terminal region, and 56–57%, 50–54% and 46–47% identity respectively with members of the three BMP subfamilies mentioned. Lower identity scores were seen with other TGF-β superfamily members. These comparisons suggest that GDF5, GDF6 and GDF7 genes define a new subgroup of BMP-related factors. Chromosome mapping has shown that the *Gdf5* locus maps between the *agouti* and *Src* loci on chromosome 2 (Fig 2). The *bp* locus has been mapped to the same region[14], identifying *Gdf5* as a candidate for the gene defective in brachypod mutants. *Gdf6* and *Gdf7* map to the proximal ends of chromosomes 4 and 12 and are not obvious candidates for other known mouse mutations (data not shown).

To test whether GDF5 is the normal product of the *bp* locus, we first isolated a full-length complementary DNA clone for the wild-type transcript. A probe from the mature region of GDF5 hybridized to a single 2.5-kilobase (kb) transcript in embryonic RNA, peaking at day 12.5 of development (data not shown). The complete sequence of a 2,329-base-pair (bp) cDNA clone of the embryonic transcript is shown in Fig. 1*b*. The wild-type sequence contains a single large open reading frame of 495 amino acids.

We next looked for alterations of *Gdf5* sequences in three independent *bp* mutations. Two of the mutations arose on the

§ To whom correspondence should be addressed.

A/J and BALB/cJ inbred mouse strains, which were included in all experiments as parental controls (Fig. 3 legend). Southern blot analysis did not detect major disruptions of *Gdf5* genomic sequences in any of the mutations; we therefore amplified coding sequences from RNA and analysed them by DNA sequencing. All three mutant alleles contained frameshift mutations in the *Gdf5* open reading frame (Fig. 3). In *bp/bp* mice, bases 477–483 of the wild-type sequence are deleted, followed by an inversion of bases 484–496. The resulting frameshift creates a translational stop codon 62 amino acids later. In bp^{3J}/bp^{3J} mice, a CG dinucleotide in the wild-type sequence is replaced by a single T at position 876. This frameshift mutation produces a translational stop at the next codon. In bp^{J}/bp^{J} mice, a stretch of three Gs in the wild-type sequence is replaced by four Gs in the mutant (positions 1,444–1,448). This change produces a stop codon 41 amino acids later. Neither sequence alteration found in the bp^{J} and bp^{3J} mutants was present in the A/J or BALB/cJ parental control strains, strongly arguing that each was the result of a new mutation at the *bp* locus.

Active signalling molecules in the TGF-β superfamily are formed from the C-terminus of a larger precursor protein[5]. The frameshift mutations in *bp*, bp^{J} and bp^{3J} all occur before the mature signalling portion of GDF5 and should represent functional null mutations. To compare the skeletal phenotypes of the different alleles, we prepared skeletons from mice homozygous for the bp^{J} and bp^{3J} mutations. As reported for the *bp* mutation on an outbred background[1,2], the new mutations on coisogenic backgrounds produce specific defects in limb morphology (Fig. 4*a*, *b*, and other data not shown). The long bones of the limb are slightly shorter, and the feet are much

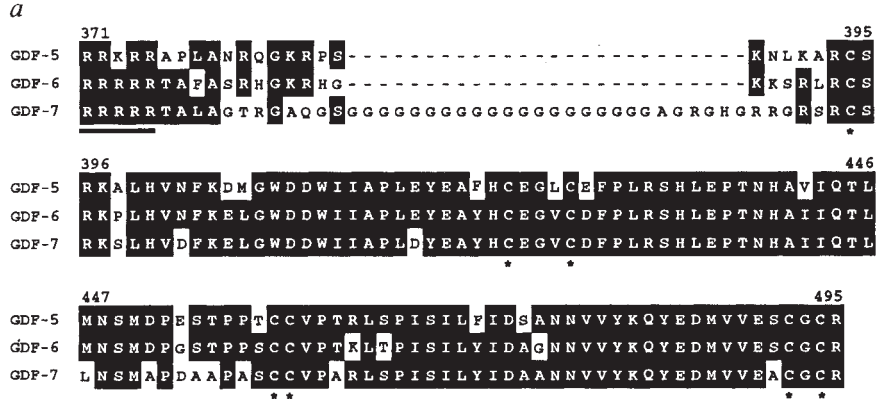

b

```
1    TTCAAGCCCTCAGTCAGTTGTGCGGGAGAAAGGGGGCGGTCGGCTTTCTCCTTTCAAGAA   60
61   CGAGTTATTTTCAGCTGCTGACTGGAGACGGTGCACGTCTGGACACGGGAGCACTTCCAC  120
121  TATGGGACTGGATACAGACACACGCCCGGCGGACTTCAAGACACTCAGACTGAGGAGAAA  180
181  GCCCTGCCTGCTGCTGCTGCTGCTGCTGCTGCACCGCTGCCTCTGAAGACCCACTCCTT  240
241  TCATGGTTTTTCCTGCCAAGCCAGAGGCACCTTCGCTGCTACGGCCTTTCTCTGTGGTGT  300
301  CATTCAGCGGCTGGCCAGAGGATGAGACTCCCCAAACTCCTCACTCTTTTGCTGTGGCAC  360
                          M  R  L  P  K  L  L  T  L  L  L  W  H
361  CTGGCTTGGCTGGACCTGGAACTCATCTGCACTGTGCTGGGTGCCCCTGACTTAGGACAG  420
     L  A  W  L  D  L  E  L  I  C  T  V  L  G  A  P  D  L  G  Q
421  AGAACCCCAGGGGCCAAGCCAGGGTTGACCAAAGCGGAGGCCAAGGAGAGGCCCACCCCTG  480
     R  T  P  G  A  K  P  G  L  T  K  A  E  A  K  E  R  P  P  L
481  GCCAGGAATGTCTTTAGGCCAGGGGGTCATATCTATGGTGTGGGGGCCACCAATGCCAGG  540
     A  R  N  V  F  R  P  G  G  H  I  Y  G  V  G  A  T  N  A  R
541  GCCAAGGGAAGCTCTGGGCAGACACAGGCCAAGAAGGATGAACCCAGAAAGATGCCCCCC  600
     A  K  G  S  S  G  Q  T  Q  A  K  K  D  E  P  R  K  M  P  P
601  AGATCCGGTGGCTCTGAAACCAAGCCAGGACCCTCTTCCCAGACTAGACAGGCTGCAGCC  660
     R  S  G  G  S  E  T  K  P  G  P  S  S  Q  T  R  Q  A  A  A
661  CGGACTGTAACCCCAAAAGGACAGCTTCCTGGGGGCAAAGCATCTTCAAAAGCAGGATCT  720
     R  T  V  T  P  K  G  Q  L  P  G  G  K  A  S  S  K  A  G  S
721  GCCCCCAGCTCCTTCCTGCTGAAGAAGACCAGGGAGCCTGGGACCCCTCGAGAGCCCAAG  780
     A  P  S  S  F  L  L  K  K  T  R  E  P  G  T  P  R  E  P  K
781  GAGCCGTTCCGCCCGCCCCCCATCACACCCCACGAATACATGCTCTCCCTGTACAGGACG  840
     E  P  F  R  P  P  P  I  T  P  H  E  Y  M  L  S  L  Y  R  T
841  CTGTCCGATGCTGACAGAAAGGGAGGTAACAGCAGCGTGAAGTTGGAGGCTGGCCTGGCC  900
     L  S  D  A  D  R  K  G  G  N  S  S  V  K  L  E  A  G  L  A
901  AACACCATCACCAGCTTTATTGACAAAGGGCAAGATGACCGAGGCCCTGCGGTCAGGAAG  960
     N  T  I  T  S  F  I  D  K  G  Q  D  D  R  G  P  A  V  R  K
961  CAGAGGTACGTGTTTGACATCAGTGCCTTGGAGAAGGATGGGCTGTTGGGGGCTGAACTG 1020
     Q  R  Y  V  F  D  I  S  A  L  E  K  D  G  L  L  G  A  E  L
1021 CGGATCTTACGGAAGAAGCCCTTGGACGTGGCCAAGCCAGCGGTCCCCAGTAGCGGGCGG 1080
     R  I  L  R  K  K  P  L  D  V  A  K  P  A  V  P  S  S  G  R
1081 GTTGCCCAACTGAAGCTGTCCAGCTGCCCCAGCGGCCGGCAGCCGGCAGCCTTGCTGGAT 1140
     V  A  Q  L  K  L  S  S  C  P  S  G  R  Q  P  A  A  L  L  D
1141 GTGCGCTCCGTGCCAGGCCTGGATGGATCTGGCTGGGAGGTGTTCGACATCTGGAAGCTC 1200
     V  R  S  V  P  G  L  D  G  S  G  W  E  V  F  D  I  W  K  L
1201 TTCCGAAATTTAAGAACTCAGCGCAGCTGTGCCTGGAGCTGGAGCCTGGGGCCTGGGGC 1260
     F  R  N  F  K  N  S  A  Q  L  C  L  E  L  E  A  W  E  R  G
1261 CGGGCCGTGGACCTCCGTGGCCTGGGCTTTGAACGCACTGCCCGACAGGTCCACGAGAAA 1320
     R  A  V  D  L  R  G  L  G  F  E  R  T  A  R  Q  V  H  E  K
1321 GCCTTGTTCCTAGTGTTTGGTCGTACCAAGAAACGGGACCTGTTCTTTAATGAGATTAAG 1380
     A  L  F  L  V  F  G  R  T  K  K  R  D  L  F  F  N  E  I  K
1381 GCCCGCTCTGGCCAGGATGACAAGACTGTGTATGAATATTTGTTCAGCCAGCGGCGGAAA 1440
     A  R  S  G  Q  D  D  K  T  V  Y  E  Y  L  F  S  Q  R  R  K
1441 CGCCGGGGCCCCATTGGCCAATCGCCAGGGCAAGCGACCCAGCAAGAACCTCAAGGCTCGC 1500
     R  R  A  P  L  A  N  R  Q  G  K  R  P  S  K  N  L  K  A  R
1501 TGCAGTCGCAAGGCCTTGCATGTCAACTTCAAGGACATGGGCTGGGACGACTGGATCATC 1560
     C  S  R  K  A  L  H  V  N  F  K  D  M  G  W  D  D  W  I  I
1561 GCACCTCTTGAGTATGAGGCCTTCCACTGCGAAGGACTGTGTGAGCTCCCCTTGCGCTCC 1620
     A  P  L  E  Y  E  A  F  H  C  E  G  L  C  E  F  P  L  R  S
1621 CACTTGGAGCCCACAAACCACGCAGTCATTCAGACCCTAATGAACTCTATGGACCCTGAA 1680
     H  L  E  P  T  N  H  A  V  I  Q  T  L  M  N  S  M  D  P  E
1681 TCCACACCACCCACTTGTTGTGTGCCTACACGGCTGAGTCCTATTAGCATCCTCTTCATC 1740
     S  T  P  P  T  C  C  V  P  T  R  L  S  P  I  S  I  L  F  I
1741 GACTCTGCCAACAACGTGGTGTATAAACAGTACGAGGACATGGTCGTGGAATCTTGTGGC 1800
     D  S  A  N  N  V  V  Y  K  Q  Y  E  D  M  V  V  E  S  C  G
1801 TGCAGGTAGCAGCACCGGCCCACCTGTCTTCCAGGGTGGCACATCCAGAGACTACCCCCT 1860
     C  R  *
1861 CTACAGGTTCCTGGAGTAACAGAGAGCCTGTGAAGCTGCTGCCCGAAGTTTCCTGGCAGC 1920
1921 CTGCAGGAAAGAGTTCTCAGCAGGCTTACTCTCTGGATGTGATCTGGACTAAAGAGATCA 1980
1981 CCTTCTGAAGATTCCTGCCCAAGGAACAGACTCTGAGTGGGCCTGGGGCTCAGGAAAGGT 2040
2041 GTTCTTAATGAGATTCAGTTCACCATCTCTCCTGCCGGGGCCGGAGACCTTCATTTCTCT 2100
2101 CCAGACTCTCCAGAGAAGTTGTAGCTATATCCTAAGCTCTTTAAGGGAGAGCTGTCTCCT 2160
2161 CCTTGAATCACCTTTGTGCCTGGTGACTTTCTGCCACGAGATGTTCATTACAGGGGCTGG 2220
2221 GCAAAGAAGGGGAAAGGGCTTGGGCAGGGGTGAAGAGAAGAGTATGAGCCTAATTAGACT 2280
2281 GTTAGATTAAAATGTACATCGATGACATAAAAGCTGAATCTTCATGGCT 2329
```

FIG. 1 Sequences of three new members of the TFG-β superfamily. *a*, Partial amino-acid sequences of GDF5, GDF6 and GDF7 are aligned beginning at their predicted protease recognition sites (underlined). Dashes denote gaps introduced to maximize the alignment. Numbers indicate amino-acid positions in GDF5. The seven conserved cysteine residues are indicated (*). Identical amino acids are shaded. *b*, Nucleotide sequence of a full-length *Gdf5* cDNA clone. The predicted GDF5 product is a 495-amino-acid, 54.9K protein with a putative proteolytic processing site (shaded box) preceding a 120-amino-acid, 13.6K mature C-terminal polypeptide. A single *N*-linked glycosylation site is located in the pro-region (open box). An in-frame termination codon upstream of the putative ATG initiation codon is underlined. The poly(A) tail is not shown.

METHODS. The following oligonucleotide primers were used to screen mouse genomic DNA for new members of the TFG-β superfamily by PCR. Corresponding amino-acid sequences are shown in brackets. SJL136: CCGGAATTCGG(G/A/T/C)TGGGA(G/A)(A/C)G(G/A/T/C)TGG(G/A)T(G/A/T/C)(G/A)T [GWE(R/S)W(V/I/M)(V/I/M)]; SJL121: CCGGAATTC(G/A)-CAICC(G/A)CA(T/C)TC(G/A)TCIACIACCAT(G/A)TC(T/C)TC(G/A)TA [reverse complement: YEDMVVDECGC]; SJL141: CCGGAATTCGGITGG(G/C/A)A-(G/A/T/C)(A/G)A(T/C)TGG(A/G)TI(A/G)TI(T/G)CICC [GW(H/Q/N/K/D/E)-(D/N)W(V/I/M)(V/I/M)(A/S)P]; SJL145: CCGGAATTC(G/A)CAI(G/C)C(G/A)CAIG(C/A)(G/A/T/C)TCIACI(G/A)(T/C)CAT [reverse complement: M(V/I/M/T/A)V(D/E)(A/S)C(G/A)C]; and SJL146: CCGGAATTC(G/A)CAI(G/C)C-(G/A)CAIG(C/A)(G/A/T/C)C(G/T)IACI(G/A)(T/C)CAT [reverse complement: M(V/I/M/T/A)V(R/S)(A/S)C(G/A)C]. PCR was carried out at 94 °C for 1 min, 50 °C for 2 min, and 72 °C for 2 or 3.5 min for 40 cycles with 2 μg CD-1 mouse genomic DNA as template. Initial GDF5, GDF6 and GDF7 sequences were identified using primers SJL136 and SJL121, SJL141 and SJL145, and SJL141 and SJL146, respectively. The GDF6 and GDF7 sequences were used to screen a mouse BALB/c genomic library from A. Lanahan. GDF5 sequences were used to screen a cDNA library constructed in the λZAPII vector (Stratagene) from day 12.5 post-coitum (p.c.) CD-1 mouse embryo poly(A)$^+$ RNA. PCR products, genomic clones and the longest cDNA clone were sequenced as described[20].

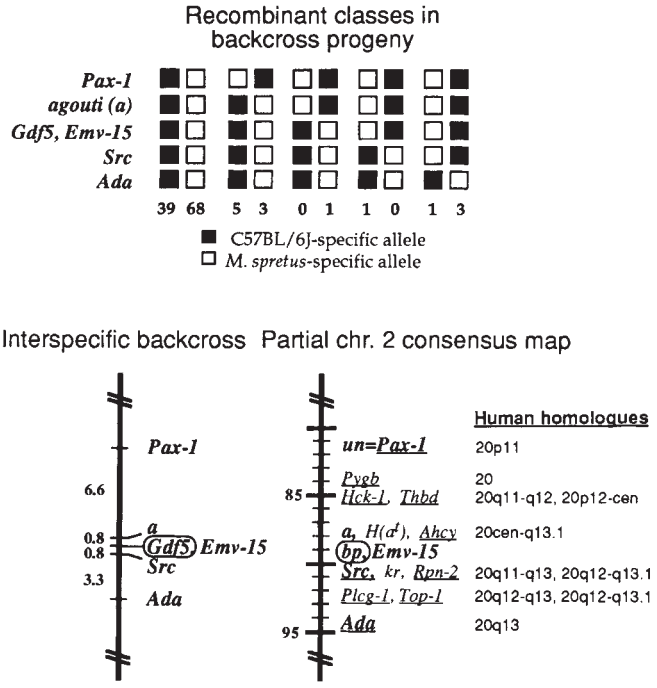

FIG. 2 *Gdf5* maps in the *bp* region of mouse chromosome 2. Top, recombination mapping places *Gdf5* between the *agouti* and *Src* loci on chromosome 2, closely linked to *Emv-15;* bottom, comparison of *Gdf5* map position with a partial consensus linkage map of distal mouse chromosome 2 (ref. 14). The *bp* locus has also been placed between *agouti* and *Src*, closely linked to *Emv-15*. Several underlined loci both proximal and distal to this region have been mapped to chromosome 20 in humans (map locations shown on the right)[14].
METHODS. DNA was prepared from progeny of an interspecific backcross between (C57BL6J × *M. spretus*) F_1 females and C57BL/6J males, digested with *Hin*cII, and analysed by Southern blot hybridization with a *Gdf5* cDNA probe (nucleotides 1,997–2,329). This probe hybridized to a 3.7-kb *Hin*cII fragment in C57BL/6J DNA, a 2.6-kb fragment in *M. spretus* DNA, and to one or both fragments in backcross progeny. The inheritance of this restriction-fragment length polymorphism in 121 backcross progeny was compared with the inheritance patterns of over 2,000 other markers previously typed on the same animals[21], including *Pax-1, a, Emv-15, Src* and *Ada*[22,23]. Columns of black and white boxes represent chromosome types inherited from the F_1 hybrid parent. Numbers beneath the columns represent the number of backcross progeny observed with each chromosome type.

shorter than controls. The reduction in length of the feet is largely the result of altered patterning of segments in the digits. In place of the proximal and medial phalanges is a single bone that has been described previously as resulting from a fusion of the proximal and medial phalangeal condensations (Fig. 4*b*)[2]. Additional defects in the length of the metacarpals and metatarsals and slight disorganization of the carpals and tarsals are also present. In contrast, the axial skeleton is largely unaffected by the mutations.

Previous studies have shown that defects in brachypod mice are first detectable around day 12 of gestation[2], when mesenchyme first aggregates into outlines of future digit elements. Digit condensations in brachypod mice are thin, malformed, and slow to initiate chondrogenesis. In addition, mesenchyme from brachypod mice shows a reduced ability to form aggregates and cartilaginous nodules *in vitro*[9,15]. To determine the sites of *Gdf5* expression in wild-type embryos, serial sections of day-12.5 embryos were analysed by *in situ* hybridization. *Gdf5* transcripts were detected in the limbs in distal precartilaginous mesenchymal condensations and in the perichondrium of more proximal skeletal structures (Fig. 4*c–f*). No other major sites of hybridization were detected in axial skeletal structures or soft tissues.

The sequencing studies reported here provide strong genetic evidence that the skeletal alterations in *bp* mice are the result of mutations in *Gdf5*. This conclusion is further supported by the map location of *Gdf5*, its homology to BMPs, its specific expression in the mesenchymal condensations that give rise to the limb

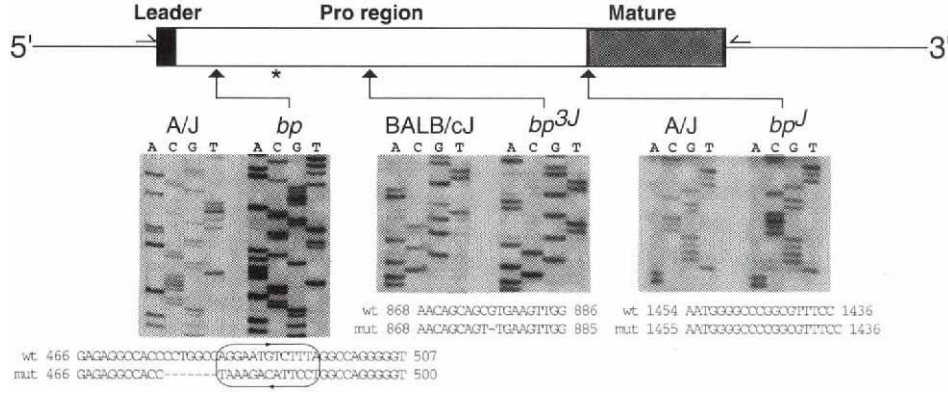

FIG. 3 Three independent *bp* mutations disrupt *Gdf5* coding sequences. Top, schematic diagram of the *Gdf5* cDNA showing positions of sequence alterations in *bp* alleles. All three mutations result in frameshifts and premature translational termination in the GDF5 open reading frame. The *bp* mutation occurred spontaneously on an outbred mouse strain in 1952[1]. The bp^J and bp^{3J} mutations occurred spontaneously in the highly inbred A/J and BALB/cJ wild-type strains in 1975 and 1993, respectively[24]. Position 613 (asterisk) is polymorphic in different strains, resulting in a serine residue in CD-1, BALB/cJ and bp^{3J} mice, and a proline residue in the A/J, bp^J and *bp* strains. Bottom, details of frameshift mutations. Wild-type and mutant sequence information is presented beneath autoradiograms demonstrating the sequence changes. The reverse complement of bases 1,436–1,454 is shown.
METHODS. *Gdf5* coding sequences were amplified from control and mutant RNA using reverse transcription and PCR. RNA was isolated from brains using RNAzol (CINNA-BIOTECX). First-strand reverse transcription reactions used primers located from 1,869 to 1,850 or 1,575 to 1,554 in the wild-type *Gdf5* cDNA sequence. cDNA reactions were then amplified with primer pairs 1,306–1,322 and 1,869–1,850, or 272–289 and 1,575–1,554. Second-round amplifications used primers 1,364–1,384 and 1,869–1,850, or 290–308 and 1,497–1,480. Amplified PCR products were cut from Sea Plaque (FMC) agarose and sequenced directly using the Sequenase Version 2.0 sequencing kit (USB). Sequencing primers correspond to positions 294–311, 767–783, 846–829, 1,364–1,384, 1,497–1,480 and 1,869–1,850 in the cDNA. Arrows bracket the region completely sequenced in two control strains and the three mutant alleles (position 320 to 1,814). Each frameshift mutation was confirmed on both strands and in at least two independent reverse-transcription PCR reactions.

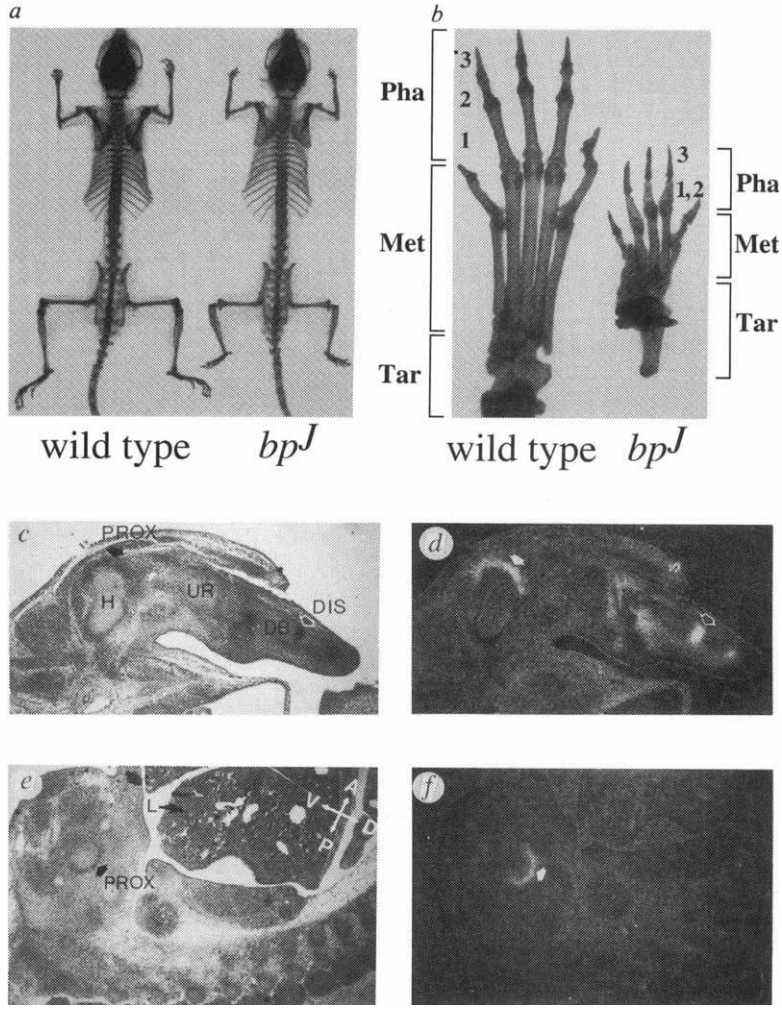

FIG. 4 Skeletal phenotype of bp^J mutant and *Gdf5* expression in the developing limb. *a*, Alizarin red skeletal preparations from a representative bp^J homozygote and an age-matched wild-type animal from the parental A/J inbred strain. The long bones are reduced and the fibula is shortened proximally. The bones of the axial skeleton are unaffected. *b*, close-up view of right hind feet. The most prominent alteration is a change in the number of the phalanges in bp^J homozygotes. In addition, metatarsals are reduced in length and the tarsals are irregular in shape. *c–f*, Expression of *Gdf5* in limb mesenchyme of day-12.5 p.c. mouse embryos. Bright-field (c, e) and dark-field (*d*, *f*) photomicrographs of transverse (*c*, *d*) and sagittal (e, *f*) sections, showing views through forelimb and posterior end of embryo, respectively, after hybridization with ^{35}S-labelled *Gdf5* antisense probe. Serial sections revealed hybridization to be localized to proximal (PROX, filled arrows) and distal (DIS, open arrows) mesenchyme in the forelimb (*c*, *d*) and hindlimb (*e*, *f*). Anterior–posterior (A–P) and dorsal–ventral (D–V) embryonic axes are indicated (e). UR, H and DB indicate primordia of ulna and radius, humerus, and digital bones; L indicates liver. *Gdf5* sense control probes produced no signals on adjacent sections (data not shown).

METHODS. Skeletons of mice were prepared in 1% (w/v) potassium hydroxide and stained using Alizarin red[25]. Day-12.5 p.c. female mouse embryos were fixed, embedded in paraffin, sectioned and hybridized as described[26] to sense or antisense RNA probes (4×10^5 c.p.m. μl^{-1}) transcribed from templates containing nucleotides 308–1,446 of the *Gdf5* cDNA clone. Slides were developed after a 4–6-week exposure time to Kodak NTB3 emulsion and were stained with haematoxylin and eosin.

skeleton, and previous experiments showing that the *bp* mutation acts cell non-autonomously in cultured cells and chimaeric mice[8,9]. The remarkable ability of BMPs to induce ectopic bone and cartilage[6] and the defects in skeletal structures caused by *Bmp5* mutations in *short ear* mice[7] has suggested that BMPs are the normal signals used to initiate bone and cartilage formation during embryonic development[16]. Our results strongly support this model and provide evidence that BMP-related genes are also required for skeletal patterning in the vertebrate limb. Strikingly, although the *brachypodism* and *short ear* mutations both disrupt the condensation of mesenchyme cells into outlines of particular skeletal elements, they do so in completely different regions of the embryo: *short ear* null mutations alter the size and shape of ears, sternum, ribs and vertebral processes, but do not alter limb bone lengths or digit morphology, whereas *bp* null mutations alter bone lengths and the number of segments in the digits of all four limbs, but do not affect ear, sternum, rib or vertebral morphology. The skeleton of higher animals thus appears to be a mosaic structure that is built from the composite patterns of activity of different BMP-like proteins. Changes in the activity of particular BMP family members may provide a general mechanism for altering the number and morphology of individual skeletal elements during development and evolution.

Although *Gdf5* transcripts are present in a variety of non-skeletal tissues in adult mice (including uterus, placenta, oviduct, brain, thymus, heart, lung, kidney and adrenal gland; data not shown), brachypod mice are fertile and do not show obvious behavioural abnormalities or striking morphological changes in soft tissues. More detailed studies will be required to determine whether subtle defects are present, or whether related family members can compensate for GDF5 deficiencies in soft tissues. A number of human brachydactyly syndromes are known that also disrupt the size or number of phalanges and limb bones without producing obvious abnormalities in other organ systems[17–19]. Direct analysis of *Gdf5* sequences or linkage studies with chromosome 20 markers (Fig. 2) can now be used to test whether any of these human syndromes are also due to *Gdf5* mutations. □

Received 26 November 1993; accepted 21 February 1994.

1. Landauer, W. *J. Hered.* **43,** 293–298 (1952).
2. Grüneberg, H. & Lee, A. J. *J. Embryol. exp. Morph.* **30,** 119–141 (1973).
3. Hinchliffe, J. R. & Johnson, D. R. *The Development of the Vertebrate Limb* (Clarendon, Oxford, 1980).
4. Johnson, D. R. *The Genetics of the Skeleton. Animal Models of Skeletal Development* (Clarendon, Oxford, 1986).
5. Massague, J. *A. Rev. Cell Biol.* **6,** 597–641 (1990).
6. Rosen, V. & Thies, R. S. *Trends Genet.* **8,** 97–102 (1992).
7. Kingsley, D. M. *et al. Cell* **71,** 399–410 (1992).
8. Malinina, N. A., Kindiakov, B. N. & Koniukhov, B. V. *Ontogenez* **15,** 514–521 (1984).
9. Owens, E. M. & Solursh, M. *Devl Biol.* **91,** 376–388 (1982).
10. Ozkaynak, E. *et al. EMBO J.* **9,** 2085–2093 (1990).
11. Celeste, A. J. *et al. Proc. natn. Acad. Sci. U.S.A.* **87,** 9843–9847 (1990).
12. Ozkaynak, E. *et al. J. biol. Chem.* **267,** 25220–25227 (1992).
13. Dickinson, M. E. *et al. Genomics* **6,** 505–520 (1990).
14. Siracusa, L. D. & Abbott, C. M. *Mamm. Genome* **4,** S31–46 (1993).
15. Elmer, W. A. & Selleck, D. K. *J. Embryol. exp. Morph.* **33,** 371–386 (1975).
16. Kingsley, D. M. *Trends Genet.* **10,** 16–21 (1994).
17. Temtamy, S. A. & McKusick, V. A. *The Genetics of Hand Malformations* 1–619 (Liss, New York, 1978).
18. Ahmad, M., Abbas, H., Wahab, A. & Haque, S. *Am. J. med. Genet.* **36,** 292–296 (1990).
19. Osebold, W. R., Remondini, D. J., Lester, E. L., Spranger, J. W. & Opitz, J. M. *Am. J. med. Genet.* **22,** 791–809 (1985).
20. McPherron, A. C. & Lee, S.-J. *J. biol. Chem.* **268,** 3444–3449 (1993).

21. Copeland, N. G. *et al. Science* **262,** 57–66 (1993).
22. Siracusa, L. D., Buchberg, A. M., Copeland, N. G. & Jenkins, N. A. *Genetics* **122,** 669–679 (1989).
23. Siracusa, L. D. *et al. Genomics* **6,** 491–504 (1990).
24. Lane, P. W., Mobraaten, L. E. & Neleski, L. A. *List of Mutations and Mutant Stocks of the Mouse Maintained at The Jackson Laboratory* (Jackson Laboratory, Bar Harbor, ME, 1993).
25. Green, M. C. *Ohio J. Sci.* **52,** 31–33 (1952).
26. Jones, C. M., Lyons, K. M. & Hogan, B. L. *Development* **111,** 531–542 (1991).

ACKNOWLEDGEMENTS. E.E.S. and T.V.H. contributed equally to this work. We thank the MRC Radiobiology Unit and The Jackson Laboratory for *bp* mutant strains. This work was supported in part by grants from Alfred and Katherine Heller and the Clarence E. Heller Charitable Foundation, by a Lucille P. Markey Scholar award, and the NIH (D.M.K.); by NCI under contract with ABL (N.G.C. and N.A.J); and by grants from the American Cancer Society, the NIH and the Edward Mallinckrodt Jr Foundation (S.-J.L).

Ligand for FLT3/FLK2 receptor tyrosine kinase regulates growth of haematopoietic stem cells and is encoded by variant RNAs

C. Hannum, J. Culpepper, D. Campbell, T. McClanahan, S. Zurawski, J. F. Bazan, R. Kastelein, S. Hudak, J. Wagner, J. Mattson, J. Luh, G. Duda, N. Martina, D. Peterson, S. Menon, A. Shanafelt, M. Muench, G. Kelner, R. Namikawa, D. Rennick, M.-G. Roncarolo, A. Zlotnik, O. Rosnet*, P. Dubreuil*, D. Birnbaum* & F. Lee

DNAX Research Institute of Molecular and Cellular Biology, 901 California Avenue, Palo Alto, California 94304-1104, USA
*U119 INSERM, 27 Boulevard Lei Roure, 13009 Marseille, France

THE FLT3/FLK2 receptor tyrosine kinase is closely related to two receptors, c-Kit and c-Fms, which function with their respective ligands, Kit ligand and macrophage colony-stimulating factor to control differentiation of haematopoietic and non-haematopoietic cells[1–5]. FLT3/FLK2 is thought to be present on haematopoietic stem cells and found in brain, placenta and testis[3–5]. We have purified to homogeneity and partially sequenced a soluble form of the FLT3/FLK2 ligand produced by mouse thymic stromal cells. We isolated several mouse and human complementary DNAs that

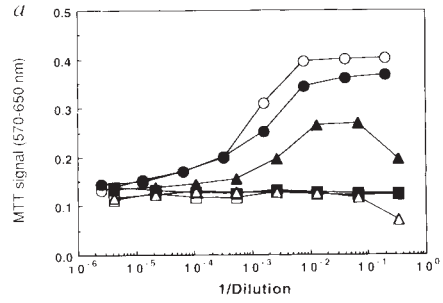

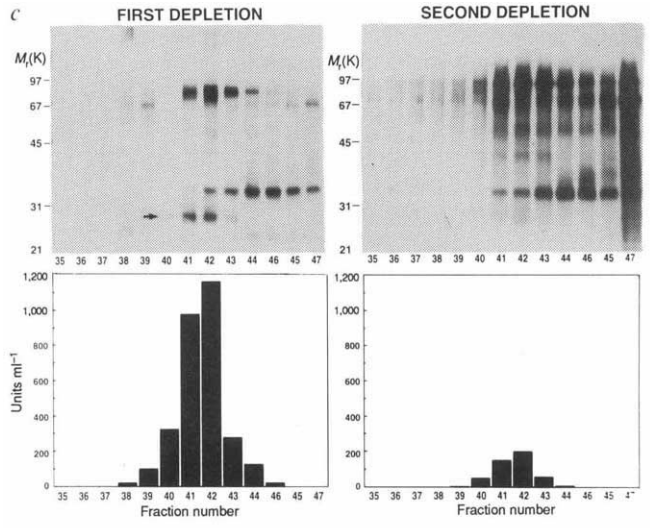

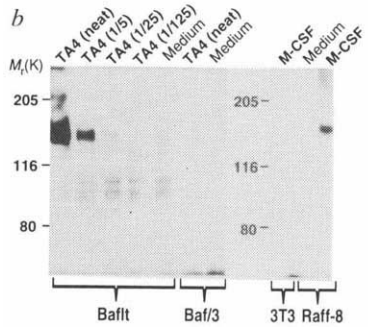

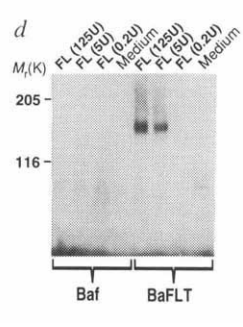

FIG. 1 FL assays and purification *a*, Survival assay (measured by 3-(4,5 dimethylthiazol-2-yl)-2,5-diphenyl tetrazolium bromide conversion) in which concentrated TA4-conditioned medium (neat, 100×) is titrated onto factor-dependent Ba/F3 (–△–) and BaFlt (–▲–) cells. Also shown is the Ba/F3 (–○–) and BaFlt (–●–) response to IL-3 and the Ba/F3 (–□–) and BaFlt (–■–) response to medium alone. *b*, Autophosphorylation assay (measured by the appearance of an immunoprecipitated FLT3 band on an antiphosphotyrosine western blot) in which TA4-conditioned medium is titrated onto Ba/F3 and BaFlt cells. As a positive control, the tyrosine-phosphorylated receptor was precipitated from M-CSF-stimulated Raff-8 cells (Rat-2 fibroblasts transfected with a chimaeric receptor composed of the ligand binding domain of c-Fms and the intracellular domain of FLT3/FLK2). *c*, Analysis of fractions from reversed-phase HPLC of affinity-purified FL from the consecutive first (left) and second (right) affinity depletions. Top, silver-stained SDS–PAGE on reduced samples of each fraction in the region of FL activity. FL is the ~30K band whose appearance coincides with biological activity. Lower, FL activity in each fraction as measured using the BaFlt-Ba/F3 survival assay. In this case fractions 40–43 from the first depletion were then combined and run on preparative SDS–PAGE (not shown) to purify the FL to homogeneity for sequence analysis. The crude TA4-conditioned medium contains about 0.05 ng FL per ml, and affinity chromatography plus RP-HPLC produces biologically active FL that is purified >300,000-fold. *d*, Autophosphorylation assay using highly purified natural FL.

METHODS. To measure FL biological activity, MTT colorimetric assays[13] were performed in parallel on Ba/F3 and BaFlt cells using 10^4 cells per well. The FL-specific dose response was calculated by subtracting the Ba/F3 titration signal from the corresponding BaFlt titration signals. Unit of FL activity, amount of active material producing 50% maximal stimulation. For receptor phosphorylation assays, 3×10^6 BaFlt or Ba/F3 cells were stimulated with ligand for 5 min. Cell lysates were prepared and immunoprecipitated with an antiserum against the kinase-insert domain of FLT3/FLK2[14]. This antiserum was also used to detect the chimaeric c-Fms/FLT3 receptor on Raff-8 cells. Immunoprecipitates were run on SDS–PAGE and western blots probed with an antiphosphotyrosine antibody (4G10). Typically >90% of the FL in 200 l of TA4-conditioned medium was adsorbed with 5 ml FLT3/FLK2 affinity beads, eluted with 0.1M glycine, pH 2.5, and chromatographed on a 4.6 × 200 mm Poros R/H (PerSeptive) reversed-phase column with a linear 28% to 40% CH_3CN gradient (into H_2O) with 0.1% TFA. Active fractions were combined and run in a single lane of an SDS–PAGE minigel. The FL band was then either blotted to PVDF membrane for direct N-terminal sequencing or excised and digested with endoproteinases (trypsin, chymotrypsin, or AspN) for sequence determination of peptides purified by microbore RP-HPLC. Sequencing was done with Applied Biosystems 476A and 477A gas phase sequencers.